RESEARCH PAPER

CrossMark

The requirements for low-temperature plasma ionization support miniaturization of the ion source

Andreas Kiontke[1] · Frank Holzer[2] · Detlev Belder[1] · Claudia Birkemeyer[1]

Abstract

Ambient ionization mass spectrometry (AI-MS), the ionization of samples under ambient conditions, enables fast and simple analysis of samples without or with little sample preparation. Due to their simple construction and low resource consumption, plasma-based ionization methods in particular are considered ideal for use in mobile analytical devices. However, systematic investigations that have attempted to identify the optimal configuration of a plasma source to achieve the sensitive detection of target molecules are still rare. We therefore used a low-temperature plasma ionization (LTPI) source based on dielectric barrier discharge with helium employed as the process gas to identify the factors that most strongly influence the signal intensity in the mass spectrometry of species formed by plasma ionization. In this study, we investigated several construction-related parameters of the plasma source and found that a low wall thickness of the dielectric, a small outlet spacing, and a short distance between the plasma source and the MS inlet are needed to achieve optimal signal intensity with a process-gas flow rate of as little as 10 mL/min. In conclusion, this type of ion source is especially well suited for downscaling, which is usually required in mobile devices. Our results provide valuable insights into the LTPI mechanism; they reveal the potential to further improve its implementation and standardization for mobile mass spectrometry as well as our understanding of the requirements and selectivity of this technique.

Introduction

The introduction of two ambient ionization techniques for atmospheric pressure mass spectrometry—DESI (desorption electrospray ionization) in 2004 [1] and DART (direct analysis in real time) [2] in 2005—made it possible to directly analyze samples with minimal or no sample preparation, potentially saving considerable time and resources. Ambient techniques

all use basically the same approach: the sample interacts by, for example, charged droplets [1, 3, 4], plasma species [2, 5, 6], or photons [7–9]. Meanwhile, a large number of techniques for the ionization of analytes under ambient conditions directly from sample surfaces have been developed. These are essentially based on minor changes to or extensions of DESI and DART. Plasma-based ambient ionization techniques are particularly fascinating due to their simple source design, solvent-free operation, and reduced waste production as compared to other ambient ionization methods (DESI and related techniques, paper spray, and others). Moreover, these ionization techniques generally produce easy-to-interpret mass spectra since the ionization mechanism commonly involves the protonation of the analyte by hydronium-ion–water clusters produced during the interaction of the atmospheric plasma with water in the surrounding air [10, 11].

Another important advantage of plasma sources is their simple yet robust construction, and many variants of such sources in terms of their geometric arrangement and the applied voltage used have been published. For instance, atmospheric pressure glow discharge (APGD) [12] and flowing atmospheric pressure

✉ Andreas Kiontke
andreas.kiontke@uni–leipzig.de

✉ Claudia Birkemeyer
birkemeyer@chemie.uni–leipzig.de

[1] Institute of Analytical Chemistry, University of Leipzig, Linnéstraße 3, 04103 Leipzig, Germany

[2] Department of Environmental Engineering, Helmholtz-Centre for Environmental Research, Permoser Str. 15, 04318 Leipzig, Germany

afterglow (FAPA) [13] utilize DC voltage, while plasma sources with dielectrics such as LTPI (low-temperature plasma ionization) or DBDI (dielectric barrier discharge ionization) [6, 14] require AC voltage. Plasma sources may also differ in the temperature applied; for instance, DART usually employs an additional heater, in FAPA and APGD temperature is increased by Joule heating resulting from plasma generation, whereas efficient ionization is achieved without the need to heat up the plasma gas in LTP/DBDI.

In contrast to the more commonly employed method of electrospray ionization [15, 16], the signal responsiveness for plasma-based techniques and its dependence on the source parameters have only rarely been investigated. There are only a few reports in which the effects of various factors on the signal intensity have been taken into consideration. For instance, the influences of the plasma gas used [6, 17, 18] and the electrode spacing in an LTP [6] on the signal intensity have been investigated, as has the dependence of the power consumption on the distance between the electrodes [19]. In addition, only a few reports contain information about practical considerations regarding the source configuration, such as the angle of the plasma source with respect to the sample [6].

For our research, we used an easy-to-build and cost-efficient plasma ionization source, the LTP probe [6]. Our goal was to identify the optimum conditions for a resource-conserving mobile plasma source. Compared to the handheld plasma probe [20], we changed the electrode configuration: instead of coaxial electrodes, we used an in-probe configuration of a DBDI plasma ion source with two parallel outer electrodes [21], since the presence of a dielectric between the electrodes and the plasma gas (helium) limits the current, resulting in a nonequilibrium low-temperature plasma [22]. Here, we present a systematic study of the influence of the source geometry and configuration on the signal intensity in mass spectrometry.

Materials and methods

Chemicals

Acetonitrile was purchased from VWR (Dresden, Germany), aniline was obtained from Acros (Geel, Belgium), water was from BIOSOLVE (Valkenswaard, Netherlands), and 4-fluoro-*o*-phenylenediamine and *o*-anisidine were from Sigma–Aldrich (Taufkirchen, Germany). Paper was purchased from UPM Paper ENA (Augsburg, Germany) and cut into 2×5 cm pieces for application as single-use targets.

Plasma source parts

The plasma source consisted of an ignition transformer (EBI4 CM S, Danfoss, Nordborg, Denmark) and a glass tube (GC

liner, Thermo Scientific, Waltham, MA, USA) with two surrounding outer electrodes made of copper foil tape (Noll GmbH, Wörrstadt, Germany). The electrodes were covered with a homemade Teflon housing. The ignition transformer converted 230 V at 50/60 Hz to a peak-to-peak voltage (V_{PP}) of 2×7.5 kV at a frequency of 25 kHz. Helium 5.0 (Air Liquide, Düsseldorf, Germany) was used as plasma gas. A photograph of the plasma source is provided in Fig. 1a.

Optical emission spectroscopy

Spectroscopic measurements were performed on an Ocean Optics USB2000 fiber optic spectrometer (operated using the OOIBase32 2.0.1.4 software package) to detect excited plasma species. The distance between the plasma source outlet and the fiber probe was one centimeter and the optical emission from the plasma discharge was recorded in the range 200–880 nm. The helium flow rate of the plasma source was 10, 20, 50, or 100 mL/min. Spectra obtained from OES (optical emission spectroscopy) of the generated plasma are shown in the "Electronic supplementary material" (ESM; Fig. S1a–d).

Instrument configuration

The optimal plasma source configuration was first assessed by determining the signal intensities of the ionized air species produced by the plasma and detected after coupling the source to an Esquire 3000+ ESI ion-trap MS (Bruker Daltonics, Bremen, Germany). A representative mass spectrum of ionized air species in the plasma source afterglow is shown in Fig. S2 of the ESM. For this investigation, the plasma source was directed towards the MS inlet (angle 0°) in a distance of 1 cm in order to obtain appropriate sensitivity (Fig. 1b). The high voltage and the nebulizing gas of the ESI ion trap were switched off and a dry gas flow rate (nitrogen) of 2 L/min at 200 °C was applied. The scan range was set to m/z 15–50 with a target mass of m/z 40.

In a second approach, to assess the influences of the distance of the sample from the MS inlet and the distance of the plasma source from the sample on the signal intensity, a 1 mM solution in 1:1 ACN/H_2O of the model compounds aniline (referred to as aniline sample), anisidine, and 4-fluoro-*o*-phenylenediamine was spotted onto a paper target. (Note that paper was chosen as a material in order to obtain a relatively uniform concentration within the sample spot and to avoid any deformation and sputtering of deposited sample drops at higher process-gas flow rates.) The plasma source was placed at an angle of 30° with respect to the sample (Fig. 1c) and the following instrumental parameters were applied: high voltage of the ESI ion source off; dry gas flow 1.5 mL/min (nitrogen) with the temperature set to 0 (readback was 42 °C); scan range m/z 50–300; target mass 120. The number of ions per scan was
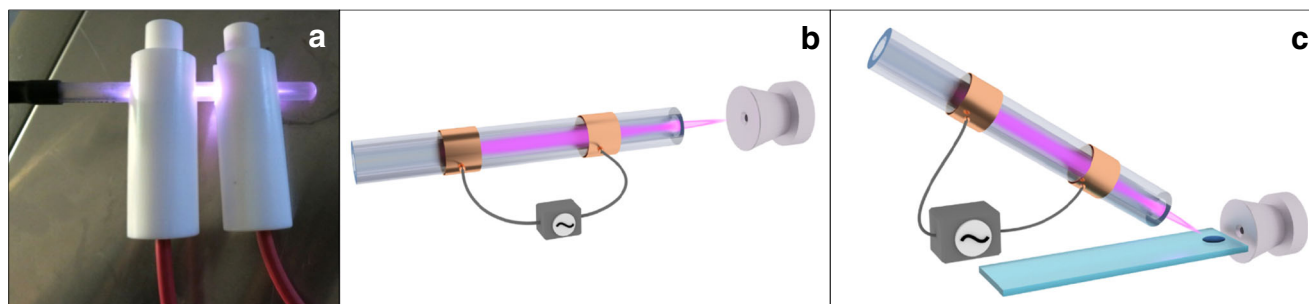
Fig. 1 **a** Photograph of the plasma source. Also shown are schematics of the plasma source **b** in front of the MS inlet and **c** directed onto a target

limited to 20,000, with a maximum accumulation time of 200 ms employed, and the rolling average of three scans taken. The acquired signal intensities were averaged over one minute of analysis time using the Bruker Data Analysis 3.3 software package, and the corresponding signal intensities of analyses performed in triplicate ($n = 3$) were used for data evaluation.

In addition, the plasma source was coupled to an API 2000 triple quadrupole mass spectrometer (AB Sciex, Toronto, Canada) in the TIS (turbo ion spray) configuration. For this purpose, the standard ESI source was removed and a self-made electronic plug (Fig. S3a in the ESM) was used to allow operation without a standard source. The following settings were used: flow rate of the plasma gas 30 mL/min; TIS voltage 0 V; source gas 1 (GS1), source gas 2 (GS2), and temperature were set to 0; curtain gas 20 psi; focusing potential 100 V; entrance potential 10 V; declustering potential 45 V. The *m/z* range was set to 65–250, with a scan duration of 3 s.

Plasma source geometry and configuration

Electrode size, shape, and arrangement as well as the process gas flow and the diameters of the dielectric were modified in various ways in order to assess the factors that most strongly influenced the ionization efficiency. The electrode widths tested were 10, 15, 20, and 25 mm (Fig. S4a in the ESM) and the distances between the electrodes tested were 45, 35, 25, and 15 mm (Fig. S4b in the ESM). For this experiment, the helium flow was kept at 30 mL/min. An optimal distance of 15 mm between the electrodes was selected for all subsequent experiments. Glass capillaries made of borosilicate glass with various outer diameters (8, 5, and 2 mm) but a constant internal diameter of 1 mm were used (Fig. S4c in the ESM) in order to investigate the influence of the dielectric strength. The process gas flow was varied between 5 and 50 mL/min. To assess the influence of the outlet distance (distance between the electrode near the MS and the "plasma outlet", i.e., the glass tube end), the electrodes were arranged at various outlet distances (20, 30, and 40 mm; Fig. S4d in the ESM). (Note that small outlet distances require particular attention to be paid to ensure proper insulation from short circuits to the MS.) The gas flow per electrode arrangement was 5, 10, 20, 30, 40, or 50 mL/min.

The influences of the distances between the plasma source, sample, and MS inlet (Fig. 2) were assessed. The distance of the plasma source to the sample was varied (either 5, 10, 15, or 20 mm) while the distance of the sample from the MS inlet was kept constant at 5 mm (Fig. 2a). The distance between the sample and MS inlet was varied (either 5, 10, 15, or 20 mm) while the plasma source was kept at a distance of 5 mm from the sample (Fig. 2b). The flow rate was kept constant at 30 mL/min.

Results and discussion

LTPI: easy to build and couple and couple to MS as ambient ionization technique?

In contrast to how easy it was to couple the plasma source to a number of ESI-MS instruments (Esquire 3000+, MicrOTOF, and Impact II; data not shown), frequent signal drops were observed when an attempt was made to couple the plasma source to the API 2000 mass spectrometer (Fig. S3b of the ESM). Within the TIS (turbo ion spray) configuration, all potentials (entrance, focusing, and declustering) were ramped to assess their relationships to the signal failures, but the situation could not be improved.

Removing the curtain plate increased the signal intensity, but it did not solve the problem of the observed signal interruptions. The LCMS-2010 from Shimadzu (Kyōto, Japan) showed similar behavior (not shown), and such periodic behavior was also observed by other authors when they used an ESI Orbitrap from Thermo Fisher Scientific (Waltham, MA, USA) [23]. The most obvious difference between these instruments and the Bruker instrument is their needle-on-potential configuration, while the plasma source probe does not provide high potential. However, the generation of an electric field between the plasma source and the MS inlet by mounting an electrode just behind the plasma source (Fig. S5 in the ESM) and applying a potential of between 0 and 5500 V did not succeed in stabilizing the signal either.

Though ESI measurements showed strong dependences of the signal response on the mass spectrometer and source configuration used [24], a stable signal was ultimately achieved
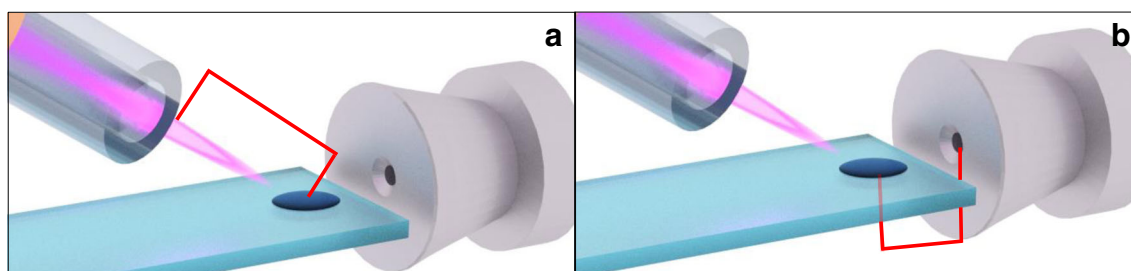
Fig. 2 Schematic drawing of the various distances that were trialed between **a** the plasma source and the sample and **b** the sample and the MS inlet

with each instrument, and the different responses were assumed to be consequences of, for example, different desolvation/solvent declustering in the differently configured ion sources. On the other hand, when solid substrate ESI (an ambient technique developed for needle-on-potential instruments that requires the application of voltage to the probe, such as a paper spray [25], wooden tip spray [26], or touch spray [27]) is applied in needle-on-ground instruments, modifications such as applying a negative potential to the MS entrance [28] and grounding the sample must be carried out [29]. The application of a potential to the sample target in a needle-on-potential instrument could eventually improve the stability of the signal, but further studies may be needed before stable LTPI coupling can be achieved reproducibly in a needle-on-potential configured instrument.

Plasma source efficiency benefits from narrow design

Many factors have been reported to influence the plasma jet and would therefore be expected to impact the ionization efficiency or signal intensity in ambient plasma ionization too; examples include the process gas flow [30], the electrode arrangement [31], and the high voltage applied [32]. Of these, we investigated the electrode width, the distance between the electrodes, the thickness of the dielectric, the distance between the electrodes and the outlet of the plasma source, the distance of the sample from the MS inlet, and the influence of the distance of the plasma source from the sample on the signal intensity.

The electrode arrangement is fairly flexible

According to Walsh and Kong [33], a linear-field setup using parallel electrodes offers more plasma activity in the downstream region compared to a coaxial setup (cross-field) as used in the Harper LTP probe [6]. Therefore, our plasma probe utilized a glass tube and two outer copper electrodes made of copper foil tape. The electrodes were connected to the power supply operating at a high voltage and high frequency (2 × 7.5 kV peak to peak at a frequency of 25 kHz), as described above in the "Materials and methods" section.

The width and distance between the electrodes were systematically altered (Fig. S4a and b in the ESM) to assess their influence on the signal intensity, while the distance of the second electrode from the plasma source outlet was kept at 20 mm at all times to ensure comparability. The sum of the intensities of the ionized plasma species (see Fig. S2 in the ESM) at a He flow rate of 30 mL/min was plotted then as a function of electrode width (Fig. 3a) or interelectrode spacing (Fig. 3b).

The intensities of the ionized plasma species detected by MS decreased slightly (by approximately 10%) upon increasing the electrode widths (Fig. 3a, RSD of three replicates <10%). This observation is in agreement with the findings of Urabe et al. in 2010, who described the influence of the electrode geometry on the intensities of plasma species, and found that parallel copper sheets yielded a shorter plasma beam with a higher density, while narrow parallel electrodes produced a longer plasma plume but a much lower density of plasma species. On the other hand, changing the distance between the electrodes did not influence the signal intensity (Fig. 3b), which is also consistent with the literature [19], as greater electrode spacing led to increased power consumption but not to an increase in signal intensity. However, when the electrode separation was too large, interruptions of the plasma occurred, as explained by Paschen's law [34], which describes the breakdown voltage as a function of plasma gas pressure. In contrast, when the electrodes were too close to each other, the risk of a short circuit dramatically increased. These results suggest a fair degree of flexibility in the design of plasma sources for mass spectrometry with respect to the electrode spacing. An electrode width of 10 mm and a distance of 15 mm between the elctrodes were used in subsequent studies.

The minimum process-gas flow rate decreases when the dielectric thickness and plasma outlet distance are decreased

The effects of the dielectric thickness and the process-gas flow were assessed by varying the dielectric thickness (4, 2, or 0.5 mm) using three different outer diameters of the glass tube (Fig. S4c in the ESM) and various helium flows of between 5 and 50 mL/min. The results are illustrated in Fig. 4a.

Fig. 3 The effect of the electrode arrangement on the plasma ionization response of air species: **a** effects of varying the width of the electrodes. **b** Effect of varying the distance between the electrodes (He flow = 30 mL/min, $n = 3$)
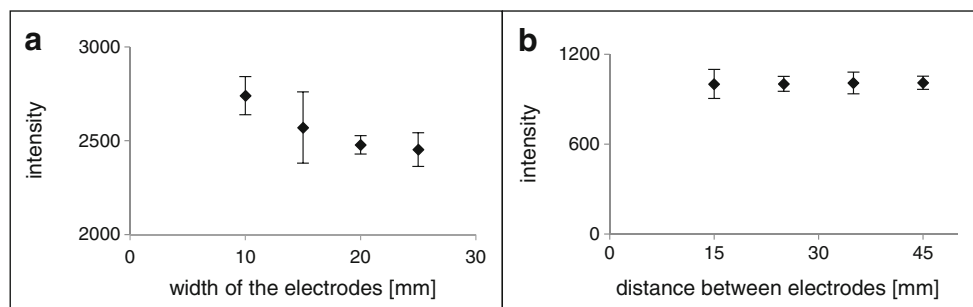
The plasma source with a dielectric thickness of 0.5 mm could not be used, even after several attempts, because heat generation caused the glass capillary to melt. The intensity profiles obtained using the two remaining dielectric thicknesses were noticeably different. While the plasma source with a thickness of 2 mm showed ionization products starting at a gas flow of 5 mL/min and an intensity plateau from 20 mL/min, the plasma source with a dielectric thickness of 4 mm showed ions only from at least 10 mL/min. At this flow rate, the signal intensity was approximately 50% of that seen for the plasma source with a dielectric thickness of 2 mm. The intensity plateau was not reached before 50 mL/min. Moreover, the intensity of the ions of this plasma source always remained below the intensity of the ions of the plasma source with the thinner dielectric, possibly due to increased charge transfer with smaller dielectric capacitances [35]. The dielectric behaves in the alternating field as a capacitor with a capacitance that increases when the dielectric thickness is decreased or the permittivity is increased. A higher capacitance results in a higher current flow, leading to a higher concentration of electronically excited species, but it also results in increased power dissipation, which causes the dielectric to heat up. Consequently, while higher ion intensities could be achieved by employing thinner dielectrics, this also results in insufficient heat dissipation, raising the temperature of the plasma source (temperature = kinetic energy of the plasma gas particles). Therefore, the efficiency of a plasma source can be enhanced by improving heat dissipation (e.g., by cooling the plasma source through the use of very thin dielectrics). In some systems, an increased plasma gas flow is used to achieve this effect, although this has the drawbacks of sample swirling and enhanced plasma gas consumption. Consequently, we recommend that other strategies should be applied when implementing thin dielectrics. For subsequent studies, a dielectric thickness of 2 mm was used.

The outlet distance (Fig. S4d in the ESM) was varied systematically to assess its influence on the signal intensity at various gas flows of between 5 and 50 mL/min. Figure 4b illustrates the total ion currents obtained for different electrode to plasma tube outlet distances at various process-gas flow rates.

The intensities show that the signal threshold varied with the outlet distance. For an outlet distance of 4 cm, no ionic species were detected in the MS for gas flows of below 20 mL/min. At this flow rate, the signal intensity was less than 50% of that for the plasma source with an outlet distance of 2 cm. Further increasing the flow rate to 50 mL/min brought a minor increase in signal intensity. For an outlet distance of 3 cm, ionized species were detected from a gas flow of 10 mL/min or higher. The signal intensity reached a value of 56% of that obtained with an outlet distance of 2 cm. Overall, intensities were higher than for the plasma source with a 4 cm outlet distance. Similarly, however, there was an increase in the intensity with higher gas flows. With an outlet distance of 2 cm, high intensities were obtained from gas flows as low as 5 mL/min. In analogy to the behavior of the signal intensity at higher flow rates, an intensity plateau was reached from about 10 mL/min onwards.

Since the intensities obtained with the various outlet distances were similar at higher flow rates, it can be reasoned that the length of the plasma jet plays a crucial role. The plasma jet must reach a minimum length in order to achieve a signal intensity plateau. Among other factors, the length of the plasma jet is influenced by the plasma process gas and voltage [32] as well as the electrode configuration [31, 33, 36], all of which were held constant, and the gas flow [30]. As a result, a lower gas flow rate can be used in conjunction with a smaller outlet spacing, since an intensity plateau is reached very quickly. Based on these findings, the smallest outlet distance that prevents flashovers to the MS entrance would be the optimal configuration. Consequently, an outlet distance of 2 cm was used in subsequent studies.

We further examined the agreement of our results for the ionized air species with those gained from the ionization of target analytes, and carried out gas-flow-dependent measurements with a 1 mM aniline solution in 1:1 ACN/H_2O. When examining the influence of the process-gas flow on the signal intensity of the ionization products from air, the plasma source was positioned horizontally in front of the MS inlet (Fig. 1b), whereas the plasma source had an optimal angle of 30° for target analysis (Fig. 1c). Ionization of the aniline sample applied to a paper target highlighted a similar dependency of signal intensity on the flow rate (Fig. S6 in the ESM) to that seen for the ionized air species. Again, the intensity increased with the flow rate. An intensity plateau was reached at about

Fig. 4 The effects of **a** the dielectric thickness and **b** the outlet distance on the plasma ionization response of ionized air species ($n = 3$)
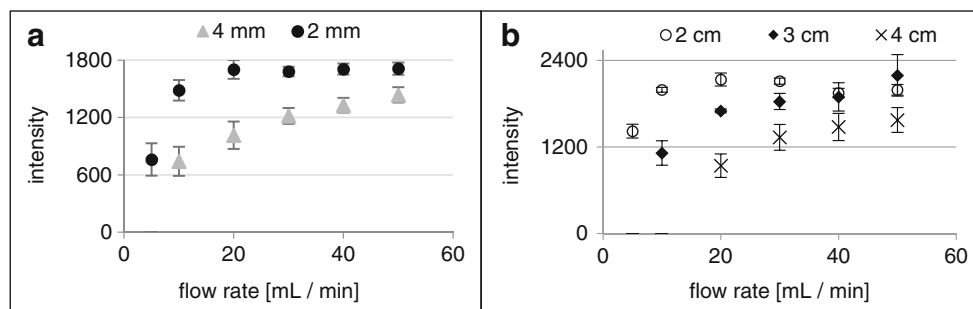
10 mL/min. In conclusion, the signal responsiveness of the target analyte was found to be related to the amount of ionized plasma species present.

The distances between the source outlet, sample, and mass spectrometer are the main determinants of signal intensity

In the second part of the study, the relationships of the signal intensity to the distance from the sample to the MS inlet (Fig. 5a) and to the distance of the plasma source from the sample (Fig. 5b) were examined using the model compounds 4-fluoro-o-phenylenediamine, o-anisidine, and aniline. Each analyte was spotted on a paper target at a concentration of 1 mM in 1:1 ACN/H$_2$O (mass spectra of the analytes are shown in Fig. S7a–c in the ESM). The intensities of the three analytes were maximum normalized and averaged to isolate the influences of the respective distances from that of the compound's responsiveness. The results are illustrated in Fig. 4 (Fig. S8 in the ESM shows the maximum-normalized signal intensities of all the analytes separately).

In both cases, a precipitous decline in signal intensity was observed with increasing distance. In the case of the distance between the sample and the MS inlet (Fig. 5a), the signal intensity at a distance of 20 mm was about one-tenth compared to a distance of 5 mm. In contrast, when the distance between the plasma source and sample was increased from 5 mm to 20 mm, the signal intensity decreased to 1/75 of its original value (Fig. 5b). We suggest that these results can be explained by the fact that the ionized target species can travel rather long distances without reacting whereas the ionizing

plasma species will react quicker with any ambient species, meaning that they cannot ionize the target analyte any further.
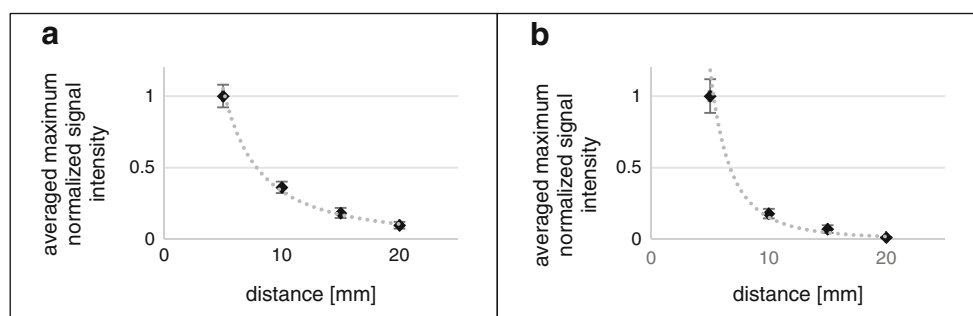
As expected, short distances seem to enhance the signal responsiveness. In particular, the distance between the plasma source and the sample should be kept small.

Conclusion

In this study, the impact of optimizing the parameters for DBDI plasma sources for mass spectrometry was assessed. Generally, signal intensity was found to improve as the distance between the plasma and the sample (including the distance between the plasma generation zone and the afterglow outlet) and the sample-to-MS inlet distance decreased. Narrow spacing also enabled the flow of the process gas to be reduced: stable signals were seen from 10 mL/min and a signal intensity plateau from a flow rate as low as 20 mL/min, which are important results from the perspective of the miniaturization of this technique and its implementation in mobile devices. In addition, reducing the dielectric thickness caused the signal intensity plateau to be reached at a lower flow rate. Optimizing all of the parameters studied in this work improved the signal intensity by as much as ~3000-fold (based on the parameter value ranges considered here).

Taking just a few geometric parameters into account, a simple, effective, and resource-conserving low-temperature plasma ionization source could be designed for application as a very promising inlet for mass spectrometry in mobile applications. Due to the advantages of downscaling the source size, such as enhanced responsiveness and reduced process-gas consumption, LTPI is an ideal technique to implement in

Fig. 5 Average maximum-normalized signal intensity of the analytes as a function of **a** the distance between the sample spot and the MS inlet and **b** the distance between the plasma source and the sample spot (He flow = 30 mL/min, $n = 3$)

mobile analytical devices in a way that conserves resources and requires minimal equipment.

Compliance with ethical standards

Conflict of interest The authors declare that there is no conflict of interest relating to this work.

References

1. Takats Z, Wiseman JM, Gologan B, Cooks RG. Mass spectrometry sampling under ambient conditions with desorption electrospray ionization. Science. 2004;306:471–3.
2. Cody RB, Laramée JA, Durst HD. Versatile new ion source for the analysis of materials in open air under ambient conditions. Anal Chem. 2005;77:2297–302.
3. Chen H, Venter A, Cooks RG. Extractive electrospray ionization for direct analysis of undiluted urine, milk and other complex mixtures without sample preparation. Chem Commun (Cambridge, UK). 2006:2042–4.
4. Haddad R, Sparrapan R, Kotiaho T, Eberlin MN. Easy ambient sonic-spray ionization-membrane interface mass spectrometry for direct analysis of solution constituents. Anal Chem. 2008;80:898–903.
5. Ratcliffe LV, Rutten FJM, Barrett DA, Whitmore T, Seymour D, Greenwood C, et al. Surface analysis under ambient conditions using plasma-assisted desorption/ionization mass spectrometry. Anal Chem. 2007;79:6094–101.
6. Harper JD, Charipar NA, Mulligan CC, Zhang X, Cooks RG, Ouyang Z. Low-temperature plasma probe for ambient desorption ionization. Anal Chem. 2008;80:9097–104.
7. Shiea J, Huang M-Z, Hsu H-J, Lee C-Y, Yuan C-H, Beech I, et al. Electrospray-assisted laser desorption/ionization mass spectrometry for direct ambient analysis of solids. Rapid Commun Mass Spectrom. 2005;19:3701–4.
8. Sampson JS, Hawkridge AM, Muddiman DC. Generation and detection of multiply-charged peptides and proteins by matrix-assisted laser desorption electrospray ionization (MALDESI) Fourier transform ion cyclotron resonance mass spectrometry. J Am Soc Mass Spectrom. 2006;17:1712–6.
9. Nemes P, Vertes A. Laser ablation electrospray ionization for atmospheric pressure, in vivo, and imaging mass spectrometry. Anal Chem. 2007;79:8098–106.
10. Olenici-Craciunescu SB, Michels A, Meyer C, Heming R, Tombrink S, Vautz W, et al. Characterization of a capillary dielectric barrier plasma jet for use as a soft ionization source by optical emission and ion mobility spectrometry. Spectrochim Acta Part B. 2009;64:1253–8.
11. Chan GC-Y, Shelley JT, Wiley JS, Engelhard C, Jackson AU, Cooks RG, et al. Elucidation of reaction mechanisms responsible for afterglow and reagent-ion formation in the low-temperature plasma probe ambient ionization source. Anal Chem. 2011;83:3675–86.
12. Andrade FJ, Wetzel WC, Chan GC-Y, Webb MR, Gamez G, Ray SJ, et al. A new, versatile, direct-current helium atmospheric-pressure glow discharge. J Anal At Spectrom. 2006;21:1175.
13. Andrade FJ, Shelley JT, Wetzel WC, Webb MR, Gamez G, Ray SJ, et al. Atmospheric pressure chemical ionization source. 2. Desorption-ionization for the direct analysis of solid compounds. Anal Chem. 2008;80:2654–63.
14. Na N, Zhao M, Zhang S, Yang C, Zhang X. Development of a dielectric barrier discharge ion source for ambient mass spectrometry. J Am Soc Mass Spectrom. 2007;18:1859–62.
15. Golubović J, Birkemeyer C, Protić A, Otašević B, Zečević M. Structure–response relationship in electrospray ionization-mass spectrometry of sartans by artificial neural networks. J Chromatogr A. 2016;1438:123–32.
16. Abburi R, Kalkhof S, Oehme R, Kiontke A, Birkemeyer C. Artifacts in amine analysis from anodic oxidation of organic solvents upon electrospray ionization for mass spectrometry. Eur J Mass Spectrom. 2012;18:301–12.
17. Na N, Zhang C, Zhao M, Zhang S, Yang C, Fang X, et al. Direct detection of explosives on solid surfaces by mass spectrometry with an ambient ion source based on dielectric barrier discharge. J Mass Spectrom. 2007;42:1079–85.
18. Huang G, Xu W, Visbal-Onufrak MA, Ouyang Z, Cooks RG. Direct analysis of melamine in complex matrices using a handheld mass spectrometer. Analyst. 2010;135:705–11.
19. Liu Y, Ma X, Lin Z, He M, Han G, Yang C, et al. Imaging mass spectrometry with a low-temperature plasma probe for the analysis of works of art. Angew Chem Int Ed Engl. 2010;49:4435–7.
20. Wiley JS, Shelley JT, Cooks RG. Handheld low-temperature plasma probe for portable "point-and-shoot" ambient ionization mass spectrometry. Anal Chem. 2013;85:6545–52.
21. Hayen H, Michels A, Franzke J. Dielectric barrier discharge ionization for liquid chromatography/mass spectrometry. Anal Chem. 2009;81:10239–45.
22. Kogelschatz U. Dielectric-barrier discharges: their history, discharge physics, and industrial applications. Plasma Chem Plasma Process. 2003;23:1–46.
23. Hagenhoff S, Franzke J, Hayen H. Determination of peroxide explosive TATP and related compounds by dielectric barrier discharge ionization-mass spectrometry (DBDI-MS). Anal Chem. 2017;89:4210–5.
24. Kiontke A, Oliveira-Birkmeier A, Opitz A, Birkemeyer C. Electrospray ionization efficiency is dependent on different molecular descriptors with respect to solvent pH and instrumental configuration. PLoS One. 2016;1:e0167502.
25. Liu J, Wang H, Manicke NE, Lin J-M, Cooks RG, Ouyang Z. Development, characterization, and application of paper spray ionization. Anal Chem. 2010;82:2463–71.
26. Hu B, So P-K, Chen H, Yao Z-P. Electrospray ionization using wooden tips. Anal Chem. 2011;83:8201–7.
27. Kerian KS, Jarmusch AK, Cooks RG. Touch spray mass spectrometry for in situ analysis touch spray mass spectrometry for in situ analysis of complex samples. Analyst. 2014;139:2714–20.
28. Meher AK, Chen Y-C. Tissue paper assisted spray ionization mass spectrometry. RSC Adv. 2015;5:94315–20.
29. Quinn KD, Cruickshank CI, Wood TD. Ultra high-mass resolution paper spray by Fourier transform ion cyclotron resonance mass spectrometry. Int J Anal Chem. 2012;2012:382021.
30. Karakas E, Koklu M, Laroussi M. Correlation between helium mole fraction and plasma bullet propagation in low temperature plasma jets. J Phys D Appl Phys. 2010;43:155202.

31. Urabe K, Ito Y, Sakai O, Tachibana K. Interaction between dielectric barrier discharge and positive streamer in helium plasma jet at atmospheric pressure. Jpn J Appl Phys. 2010;49:106001.

32. Joh HM, Kim SJ, Chung TH, Leem SH. Comparison of the characteristics of atmospheric pressure plasma jets using different working gases and applications to plasma–cancer cell interactions. AIP Adv. 2013;3:92128.

33. Walsh JL, Kong MG. Contrasting characteristics of linear-field and cross-field atmospheric plasma jets. Appl Phys Lett. 2008;93: 111501.

34. Pedersen PO. Über den elektrischen Funken. I. Teil: Funkenverzögerung. Ann Phys. 1923;376:317–76.

35. Grove TT, Masters MF, Miers RE. Determining dielectric constants using a parallel plate capacitor. Am J Phys. 2005;73:52–6.

36. Humud HR, Obayes TK, Abbas QA. Electrodes configuration effect on some properties of low temperature plasma jet (LTPJ). IJCET. 2004;4:2580–4.